

# Giant Electric Field Tuning of Magnetic Properties in Multiferroic Ferrite/Ferroelectric Heterostructures

By Ming Liu, Ogheneyunume Obi, Jing Lou, Yajie Chen, Zhuhua Cai, Stephen Stoute, Mary Espanol, Magnum Lew, Xiaodan Situ, Kate S. Ziemer, Vince G. Harris, and Nian X. Sun\*

Multiferroic heterostructures of  $\text{Fe}_3\text{O}_4/\text{PZT}$  (lead zirconium titanate),  $\text{Fe}_3\text{O}_4/\text{PMN-PT}$  (lead magnesium niobate-lead titanate) and  $\text{Fe}_3\text{O}_4/\text{PZN-PT}$  (lead zinc niobate-lead titanate) are prepared by spin-spray depositing  $\text{Fe}_3\text{O}_4$  ferrite film on ferroelectric PZT, PMN-PT and PZN-PT substrates at a low temperature of  $90^\circ\text{C}$ . Strong magnetoelectric coupling (ME) and giant microwave tunability are demonstrated by a electrostatic field induced magnetic anisotropic field change in these heterostructures. A high electrostatically tunable ferromagnetic resonance (FMR) field shift up to 600 Oe, corresponding to a large microwave ME coefficient of  $67\text{ Oe cm kV}^{-1}$ , is observed in  $\text{Fe}_3\text{O}_4/\text{PMN-PT}$  heterostructures. A record-high electrostatically tunable FMR field range of 860 Oe with a linewidth of 330–380 Oe is demonstrated in  $\text{Fe}_3\text{O}_4/\text{PZN-PT}$  heterostructure, corresponding to a ME coefficient of  $108\text{ Oe cm kV}^{-1}$ . Static ME interaction is also investigated and a maximum electric field induced squareness ratio change of 40% is observed in  $\text{Fe}_3\text{O}_4/\text{PZN-PT}$ . In addition, a new concept that the external magnetic orientation and the electric field cooperate to determine microwave magnetic tunability is brought forth to significantly enhance the microwave tunable range up to 1000 Oe. These low temperature synthesized multiferroic heterostructures exhibiting giant electrostatically induced tunable magnetic resonance field at microwave frequencies provide great opportunities for electrostatically tunable microwave multiferroic devices.

## 1. Introduction

Tuning of magnetization is of great fundamental and technological importance. The tuning of magnetization for magnetic devices has typically been achieved by magnetic bias fields generated from electromagnets, which is slow, bulky, noisy, consumes excess energy, and puts severe limits on the applications of these magnetic devices. Electrostatic control of magnetization, if realized, will lead to new magnetic devices that are fast, compact and energy efficient, and can prevail in a wide variety of applications such as information storage, sensors, RF/microwave systems, and so on.<sup>[1–5]</sup>

Recently, multiferroic materials consisting of ferromagnetic/ferrimagnetic and ferroelectric phases have received much interest due to the large achievable stress/strain-mediated magnetoelectric (ME) coupling. This coupling can be realized as, for example, a dielectric polarization variation in response to an applied magnetic field, or as an induced magnetization from an external electric field. Magnetoelectric coupling in

multiferroic materials shows great promise in achieving electrostatically controllable magnetization and has resulted in novel, electrostatically tunable microwave magnetic devices such as filters, resonators and phase shifters based on multiferroic composites.<sup>[6–17]</sup>

Most recently, we have reported a new class of metallic microwave magnetic FeGaB films that have a high magnetostriction constant of 70 ppm and a narrow ferromagnetic resonance linewidth of 20 Oe at X-band.<sup>[18]</sup> A multiferroic composite of FeGaB/Si/PMN-PT was obtained by bonding FeGaB grown on a Si substrate onto an (011)-cut ferroelectric PMN-PT single crystal which exhibited anisotropic in-plane piezoelectric coefficients with a negative  $d_{31}$  of  $-1750\text{ pC N}^{-1}$  and a positive  $d_{32}$  of  $900\text{ pC N}^{-1}$ .<sup>[19]</sup> These anisotropic in-plane piezoelectric coefficients of PMN-PT provide an exceptional opportunity for achieving a large change of in-plane uniaxial anisotropy, and therefore large ferromagnetic resonance (FMR) frequency tunability via inverse magnetoelastic coupling.<sup>[20]</sup> The magnetoelectric composites showed a record high tunable ferromagnetic resonance frequency

[\*] Prof. N. X. Sun, M. Liu, O. Obi, J. Lou, Dr. Y. Chen, S. Stoute, Prof. V. G. Harris  
Center for Microwave Magnetic Materials and Integrated Circuits  
Department of Electrical and Computer Engineering  
Northeastern University  
Boston, MA 02115, (USA)  
E-mail: nian@ece.neu.edu  
Z. Cai, Prof. K. S. Ziemer  
Department of Chemical Engineering  
Northeastern University  
Boston, MA 02115 (USA)  
M. Espanol  
Science Department, The Winsor School  
Boston, MA 02215 (USA)  
M. Lew  
Wellesley Senior High School  
Wellesley, MA 02481 (USA)  
X. Situ  
Quincy High School  
Quincy, MA 02169 (USA)

DOI: 10.1002/adfm.200801907

of 900 MHz or 58%. However, the corresponding electrostatically induced effective magnetic field of approximately 30 Oe in the FeGaB layer of the FeGaB/Si/PMN-PT multiferroic composites is still relatively low<sup>[20]</sup> compared to what has been reported by other groups.<sup>[3,15–17]</sup> New multiferroic composite materials are needed in order to achieve higher electrostatically induced effective magnetic fields, which are critical for many microwave devices.

Spin-spray deposition is a wet chemical synthesis technique involving several chemical reactions for generating high quality crystalline spinel ferrite films with various compositions, such as  $(\text{Fe}, \text{M})_3\text{O}_4$  (where  $\text{M} = \text{Fe}, \text{Co}, \text{Ni}, \text{Zn}, \text{Al}, \text{Cr}, \text{Ti}$ , etc.), directly from an aqueous solution.<sup>[21,22]</sup> One unique feature of spin-spray processing is the low growth temperature, in the range of 25–90 °C, which is much lower than other ferrite films preparation methods, such as sputtering, MBE, and PLD, which all require high temperatures of 600 °C or above. In addition, spin-spray synthesized ferrite films can be deposited onto different substrates, such as ceramic, glass, metal, and so on, making these ferrite films readily integrated onto different integrated circuits and devices.<sup>[23,24]</sup> These spin-spray features provide an alternative route for preparing novel integrated multiferroic materials and devices.

Recently, we reported a nickel ferrite film directly deposited on PZT by spin-spray process.<sup>[25]</sup> Strong adhesion between the spin-spray deposited ferrite film and the ferroelectric phase PZT was obtained, and was further verified by high-resolution transmission electron microscope observations. For a strong strain/stress-mediated magnetoelectric coupling, strong interface adhesion is crucial; this is reflected by a large electric-field-induced remnant magnetization change of 10% at DC. In this work, novel multiferroic heterostructures were made by spin-spray deposition of  $\text{Fe}_3\text{O}_4$  ferrite films on polycrystalline PZT, (011) cut single crystal PMN-PT, and (011) cut single crystal PZN-PT slabs, forming  $\text{Fe}_3\text{O}_4/\text{PZT}$ ,  $\text{Fe}_3\text{O}_4/\text{PMN-PT}$ , and  $\text{Fe}_3\text{O}_4/\text{PZN-PT}$  multiferroic heterostructures. The  $\text{Fe}_3\text{O}_4/\text{PMN-PT}$  heterostructure showed a large electric field induced magnetic anisotropic field change, which resulted in a 30% change in remanence and a high electrostatically tuned ferromagnetic resonance field shift of  $\delta H_r = 600$  Oe; the  $\text{Fe}_3\text{O}_4/\text{PZN-PT}$  heterostructure showed a record-high FMR field tunable range of 860 Oe, corresponding to a ME coefficient of 108 Oe cm  $\text{kV}^{-1}$ .

## 2. Results and Discussion

### 2.1. Characterization of Spin-Spray-Deposited $\text{Fe}_3\text{O}_4$ Ferrite Film

Polycrystalline  $\text{Fe}_3\text{O}_4$  films were deposited at a low deposition temperature of 90 °C onto ferroelectric substrates of PZT, (011) cut PMN-PT and (011) cut PZN-PT to form multiferroic heterostructures.<sup>[25]</sup> Pure  $\text{Fe}_3\text{O}_4$  ferrite phase was obtained and confirmed by X-ray diffraction, as shown in Figure 1, exhibiting a polycrystalline spinel structure with no obvious preferred orientation. The magnetic properties of the  $\text{Fe}_3\text{O}_4$  ferrite film were characterized by vibrating sample magnetometry (VSM) and by a custom-made magnetostriction tester.<sup>[18]</sup> Well-defined magnetic hysteresis loops were observed when the external

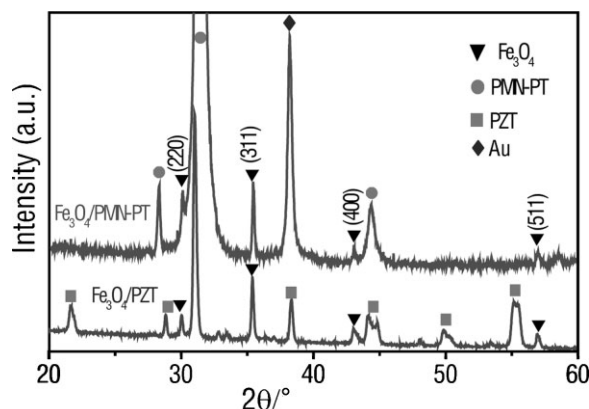


**Figure 1.** X-ray diffraction patterns of multiferroic  $\text{Fe}_3\text{O}_4/\text{PMN-PT}$  and  $\text{Fe}_3\text{O}_4/\text{PZT}$  composites.

magnetic field was applied parallel and perpendicular to the plane of the film, as shown in Figure 2, exhibiting an in-plane coercivity of 90 Oe and an out-of-plane coercivity of 110 Oe, and a saturation magnetization of the  $\text{Fe}_3\text{O}_4$  film of 410  $\text{emu cm}^{-3}$ . The magnetostriction of the  $\text{Fe}_3\text{O}_4$  film increased with the applied magnetic field and reached 28 ppm at 250 Oe, as shown in Figure 2 (inset). It is notable that the magnetostriction of the spin-spray deposited  $\text{Fe}_3\text{O}_4$  film was lower than the reported magnetostriction coefficient of 40 ppm for bulk  $\text{Fe}_3\text{O}_4$ ,<sup>[26]</sup> which could be due to the limited magnetic field strength of the magnetostriction tester. The  $\text{Fe}_3\text{O}_4$  film showed a resistivity of 6.5  $\Omega \text{ cm}$ , leading to a skin depth of about 0.5 mm when biased to have a ferromagnetic resonance (FMR) frequency at X-band. It is worth mentioning that the multiferroic heterostructures with a  $\text{Fe}_3\text{O}_4$  film on (011)-cut PMN-PT or PZN-PT slab operate in the L–T (longitudinal magnetized–transverse polarized) mode, which takes full advantages of the high in-plane permeability of the magnetic films and the large anisotropic in-plane piezoelectric constants of (011)-cut PMN-PT and PZN-PT, leading to a large tunable FMR frequency range.<sup>[20]</sup>

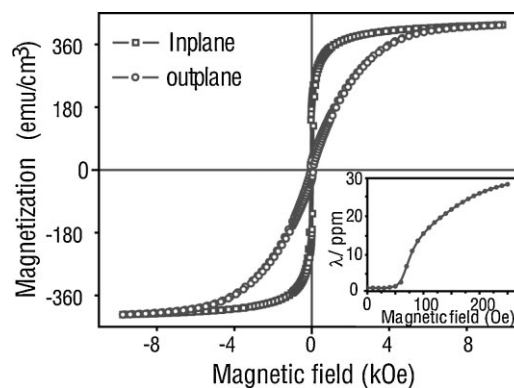


**Figure 2.** Magnetic hysteresis loops and magnetostriction curve (inset) of the  $\text{Fe}_3\text{O}_4$  ferrite film.

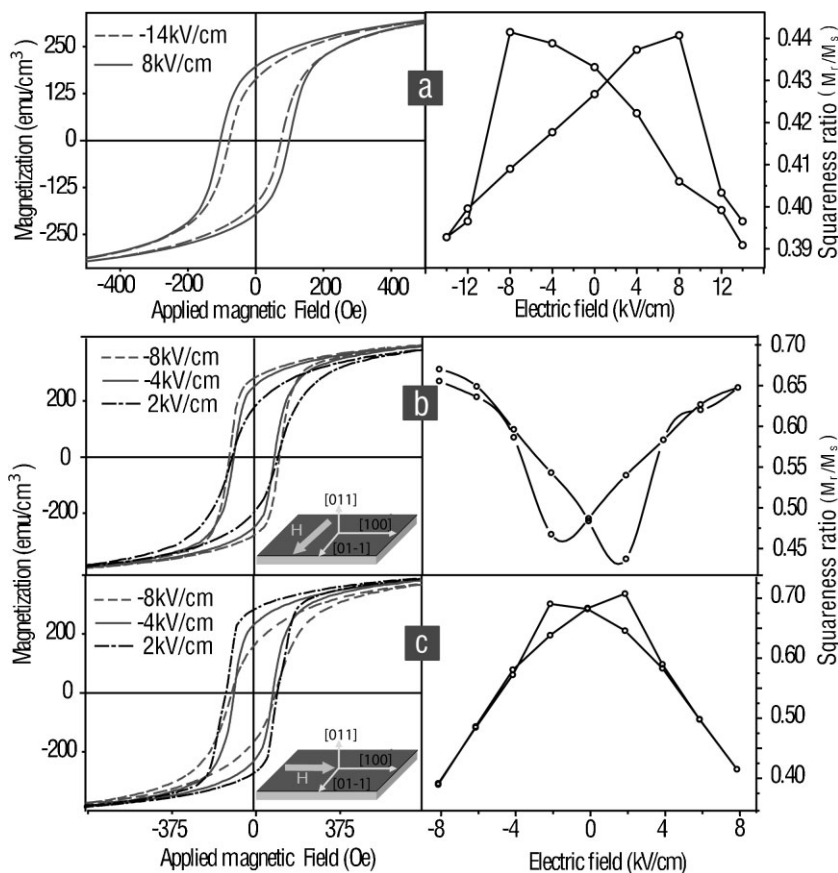


**Figure 3.** Magnetic hysteresis loops and remanence changes while external magnetic fields are along compressive stress direction ( $d_{31} = d_{32} < 0$ ) of  $\text{Fe}_3\text{O}_4/\text{PZT}$  (a), tensile stress direction  $[01\bar{1}]$  ( $d_{32}$ ) of  $\text{Fe}_3\text{O}_4/\text{PMN-PT}$  (b), and compressive stress direction  $[100]$  ( $d_{31}$ ) of  $\text{Fe}_3\text{O}_4/\text{PMN-PT}$  (c).

## 2.2. Static Magnetolectric Interaction

Static ME coupling of multiferroic heterostructures of  $\text{Fe}_3\text{O}_4/\text{PZT}$  and  $\text{Fe}_3\text{O}_4/\text{PMN-PT}$  was studied by electric-field induced changes in hysteresis loops as shown in Figure 3. The electric applied to the PMN-PT and PZT slabs led to strain in the PMN-PT and PZT substrates and in the  $\text{Fe}_3\text{O}_4$  layer. Magnetization changes were induced by the electric-field-induced strain due to the inverse magnetoelastic effect. Therefore, electric-field tuning of magnetization can be realized in the multiferroic composites through the strain/stress mediated magnetolectric coupling. As shown in Figure 3a, the in-plane magnetization process of the  $\text{Fe}_3\text{O}_4/\text{PZT}$  multiferroic composite displayed an obvious electric-field dependence of the magnetic hysteresis loops while applying electric field across the thickness of PZT. The remanence of the  $\text{Fe}_3\text{O}_4/\text{PZT}$  multiferroic composite exhibited a “butterfly” curve dependence on the electric field, with the remanence ratio tunable between 39–44%. This butterfly shape resembles the widely observed piezoelectric strain versus electric field butterfly curves for ferroelectric materials. Similar electric-dependent butterfly curves were also observed in the ferromagnetic resonance frequency and magnetization of

multiferroic composites,<sup>[20,27]</sup> indicating a strain/stress-mediated magnetolectric coupling.

The  $(011)$ -cut PMN-PT single-crystal slab has anisotropic in-plane piezoelectric coefficients of  $d_{31}$  and  $d_{32}$ , which could generate in-plane compressive stress along  $[100]$  ( $d_{31}$ ) and tensile stress along  $[01\bar{1}]$  ( $d_{32}$ ) while applying electric field parallel to  $[011]$  ( $d_{33}$ ) direction. The  $\text{Fe}_3\text{O}_4$  ferrite on PMN-PT displayed a remarkably different magnetization process when it was magnetized along the two in-plane orthogonal directions  $[01\bar{1}]$  and  $[100]$  of the PMN-PT slab, which was reflected by the opposite trend of electric field dependence of the magnetic hysteresis loops and remanence versus electric field butterfly curves, as shown in Figure 3b and c. The remanence was minimized to approximately 45% at the electric field of  $+2 \text{ kV cm}^{-1}$  and maximized to be approximately 66% at  $-8 \text{ kV cm}^{-1}$  when the external magnetic field was applied along the PMN-PT  $[01\bar{1}]$  ( $d_{32}$ ) direction. However, when the external magnetic field was applied parallel to the PMN-PT  $[100]$  ( $d_{31}$ ) direction, the remanence was maximized to approximately 70% at an electric field of  $+2 \text{ kV cm}^{-1}$  and minimized to 40% at  $-8 \text{ kV cm}^{-1}$ . It is notable that the anisotropic in-plane electric-field-induced remanence change from 40% to 70% for the  $\text{Fe}_3\text{O}_4/\text{PMN-PT}$  was much larger than the in-plane isotropic remanence change for the  $\text{Fe}_3\text{O}_4/\text{PZT}$ , and for Ni-ferrite/PZT.<sup>[25]</sup>

## 2.3. Microwave ME Interactions

Microwave ME interactions and magnetic tunabilities of spin-spray derived  $\text{Fe}_3\text{O}_4/\text{PMN-PT}$  and  $\text{Fe}_3\text{O}_4/\text{PZT}$  composites were demonstrated by electrostatic-field-induced FMR field changes at room temperature, as shown in Figure 4. Here, a microwave cavity operating at  $\text{TE}_{102}$  mode at X-band (9.5 GHz) was used to perform FMR measurements of the ferrite/ferroelectric multiferroic composites. The external bias magnetic field was applied in the  $\text{Fe}_3\text{O}_4$  film plane along the PMN-PT  $[100]$  or PMN-PT  $[01\bar{1}]$  directions, with the microwave RF field in-plane and perpendicular to the DC bias field. Clearly, giant microwave ME interaction was observed in  $\text{Fe}_3\text{O}_4/\text{PMN-PT}$ , which resulted in a high tunable FMR field range from 1185 Oe to 1786 Oe, or  $\delta H_f = 600 \text{ Oe}$ , when the electric fields across the PMN-PT thickness were changed from  $3 \text{ kV cm}^{-1}$  to  $-6 \text{ kV cm}^{-1}$  and when the external magnetic field was applied along the  $[100]$  ( $d_{31}$ ) direction of PMN-PT. This corresponded to a large microwave ME coupling coefficient of  $67 \text{ Oe cm kV}^{-1}$ . In comparison, the tunable FMR field range in  $\text{Fe}_3\text{O}_4/\text{PZT}$  was also measured as 80 Oe, which is much smaller than that of  $\text{Fe}_3\text{O}_4/\text{PMN-PT}$  due to the weak piezoelectric coefficient of PZT compared to PMN-PT.

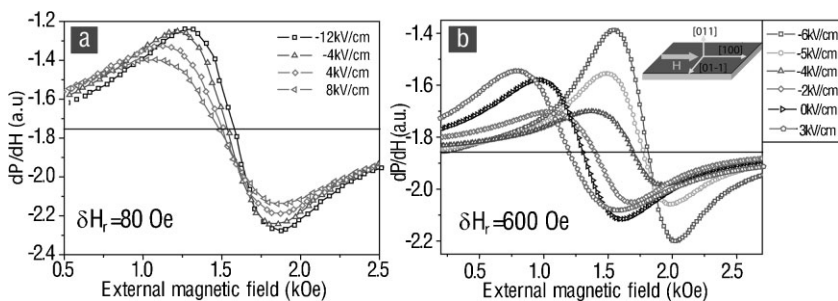


**Figure 4.** Ferromagnetic resonance absorption spectra of  $\text{Fe}_3\text{O}_4/\text{PZT}$  (a) and  $\text{Fe}_3\text{O}_4/\text{PMN-PT}$  (b) while applying different electric fields.

This electric-field-induced FMR field change can be explained by the strain-mediated electrostatic-field-induced in-plane magnetic anisotropy field  $H_{\text{eff}}$ . Depending upon whether the  $H_{\text{eff}}$  is parallel or perpendicular to the applied external magnetic field, the FMR field could be tuned up or down by electric field. The in-plane FMR frequency can be expressed by the well known Kittel equation:

$$f = \gamma \sqrt{(H_r + H_k + H_{\text{eff}})(H_r + H_k + H_{\text{eff}} + 4\pi M_s)} \quad (1)$$

where  $\gamma$  is the gyromagnetic ratio ( $\sim 2.8 \text{ MHz Oe}^{-1}$ ),  $H_r$  is the FMR field,  $H_k$  is the anisotropic field in plane,  $4\pi M_s$  is the magnetization of 5 100 G.  $H_{\text{eff}}$  is the orthogonal in-plane compressive and tensile stress corporately induced internal effective magnetic field which could be positive or negative, and can be expressed as

$$H_{\text{eff}} = \frac{3\lambda_s(\sigma_c - \sigma_t)}{M_s} \quad (2)$$

where

$$\sigma_c = \frac{Y}{1 - \nu^2} (\nu d_{32} + d_{31}) E \quad (3)$$

and

$$\sigma_t = \frac{Y}{1 - \nu^2} (d_{32} + \nu d_{31}) E \quad (4)$$

are compressive and tensile stress generated by electric field  $E$  and derived from Hooke's law for plane stress, assuming nonexistence of out-plane stress and only two orthogonal in-plane stresses coexistence;  $Y$  is Young's Modulus of  $\text{Fe}_3\text{O}_4$  ( $2.3 \times 10^{12} \text{ dyne cm}^{-2}$ ),  $\nu$  is Poisson's ratio (0.3);  $d_{31}$ ,  $d_{32}$  are  $-1750 \text{ pC N}^{-1}$  along [100] direction and  $900 \text{ pC N}^{-1}$  along [01-1] direction for (011) cut PMN-PT;  $\lambda_s$  is the saturate magnetostriction constant of 28 ppm. Theoretical calculations indicate an induced magnetic anisotropy field in the  $\text{Fe}_3\text{O}_4$  film of

approximately 670 Oe with an applied electric field of  $\pm 6 \text{ kV cm}^{-1}$ , which is comparable to the observed FMR field shift of 600 Oe. This giant microwave ME interactions, which resulted in large FMR field tunability at microwave frequencies, could lead to novel ME devices.

The FMR fields of the  $\text{Fe}_3\text{O}_4/\text{PZT}$  and  $\text{Fe}_3\text{O}_4/\text{PMN-PT}$  multiferroic composites exhibit the characteristic butterfly shape in their FMR field versus electric field curves as shown in Figure 5, which coincides with the ferroelectric hysteresis loops of the PZT and PMN-PT, and were similar to those observed in the  $\text{FeGaB}/\text{PMN-PT}$ .<sup>[20]</sup> This once again confirms that the change of FMR field of the  $\text{Fe}_3\text{O}_4$  film was resulted from the electric-field induced stress in piezoelectric and ferrite film.

#### 2.4. New Concept to Enhance Microwave Tunability

It can be concluded from Equation 1 that the FMR frequency in the  $\text{Fe}_3\text{O}_4/\text{PMN-PT}$  can be shifted upward or downward, depending on whether the applied magnetic field is parallel or perpendicular to the effective magnetic field induced by the electric field across the (011)-cut PMN-PT, which is a natural result of the anisotropic piezoelectric coefficient of the (011)-cut PMN-PT. Considering the anisotropic in-plane piezoelectric coefficients of the (011)-cut PMN-PT, which can generate orthogonal tensile and compressive stresses under an electric field, a new concept is introduced that FMR frequency could be tuned up or down and achieve a larger tunable range by applying the external magnetic field parallel to [100] ( $d_{31}$ ) or [01-1] ( $d_{32}$ ) direction of the (011)-cut PMN-PT. This idea was demonstrated in the  $\text{Fe}_3\text{O}_4/\text{PMN-PT}$  multiferroic composite. As shown in Figure 6, an external magnetic field applied along the [01-1] direction led to a reduced FMR field of 1 200 Oe (Fig. 6a). When the external field was parallel to the [100] direction, the FMR fields were shifted up to 2 200 Oe (Fig. 6b). Each of them had the same resonance field of 1 680 Oe at zero electric field due to the in-plane isotropic magnetic property of the  $\text{Fe}_3\text{O}_4$  film. The total resonance field shift was  $\delta H_r = 1 000 \text{ Oe}$  when the external magnetic field was applied parallel to [100] and [01-1] directions (Fig. 6c). This constitutes a simple but effective approach for achieving twice the

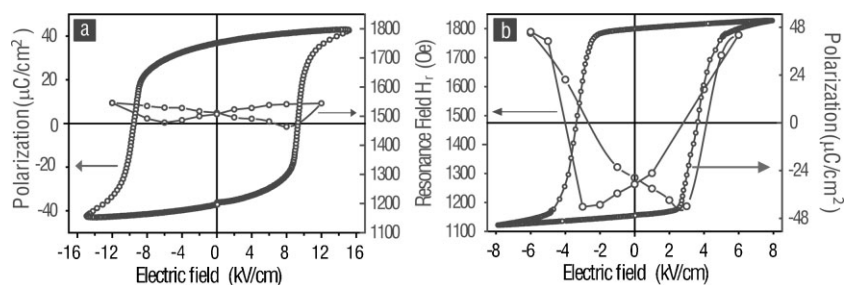


**Figure 5.** "Butterfly" curves of resonance fields versus electric fields and ferroelectric hysteresis loops of multiferroic composite  $\text{Fe}_3\text{O}_4/\text{PZT}$  (a) and  $\text{Fe}_3\text{O}_4/\text{PMN-PT}$  (b).

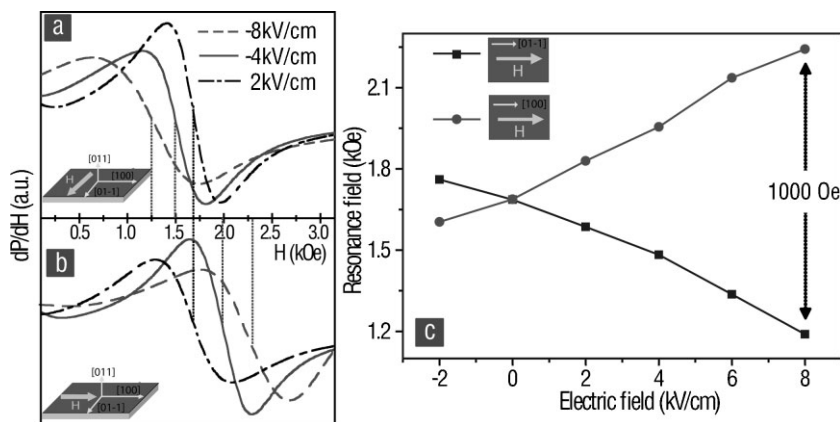


**Figure 6.** Ferromagnetic resonance absorption spectra shifts while the external magnetic field along tensional (a) and compressive (b) directions of PMN-PT. The cooperation of magnetic orientation and electric field generated resonance field change shift is up to 1000 Oe (c).

tunable FMR frequency range, leading to new opportunities of magnetostatically tunable magnetic device design with large effective magnetic field tunability.

### 2.5. Improved Tunable Magnetic Field Range and Reduced FMR Linewidth in Fe<sub>3</sub>O<sub>4</sub>/PZN-PT Heterostructures

It is notable that, while a large electrostatically tunable magnetic field of 600 Oe is observed in the Fe<sub>3</sub>O<sub>4</sub>/PMN-PT heterostructures, the FMR linewidth at X-band for the Fe<sub>3</sub>O<sub>4</sub>/PMN-PT multiferroic heterostructures is still too high, approximately 620 Oe at zero electric field and 480 Oe at a large electric field in the PMN-PT. This leads to a relatively low ratio of tunable FMR field over FMR linewidth of approximately 1, which is an important figure of merit for many tunable microwave devices (for example, a ratio of 4 has been demonstrated in YIG/PMN-PT<sup>[3]</sup>).

In order to achieve larger ratio of tunable FMR field over FMR linewidth, Fe<sub>3</sub>O<sub>4</sub> ferrite films were also spin-spray deposited onto the (011)-cut PZN-PT single crystal substrate which has a higher piezoelectric coefficient and lower loss tangent compared to PMN-PT. The microwave and static ME coupling of the Fe<sub>3</sub>O<sub>4</sub>/PZN-PT heterostructures were investigated, and the results

when external magnetic field was along [100] direction and 8 kV cm<sup>-1</sup> external electric field was applied across the thickness of PZN-PT, which was also higher than that for the Fe<sub>3</sub>O<sub>4</sub>/PMN-PT.

### 3. Conclusion

In summary, giant electric field tuning of magnetic properties were observed in spin-spray deposited Fe<sub>3</sub>O<sub>4</sub>/PMN-PT and Fe<sub>3</sub>O<sub>4</sub>/PZN-PT multiferroic composites. A high electrostatic-field-induced ferromagnetic resonance field change, or effective magnetic anisotropy field change of 600 Oe was obtained in Fe<sub>3</sub>O<sub>4</sub>/PMN-PT, corresponding to microwave ME coefficient of 67 Oe cm kV<sup>-1</sup>. A new concept was brought forth to significantly enhance the microwave resonance field tunable range up to 1000 Oe by switching the external magnetic field direction with respect to the crystallographic orientation of the (011) cut PMN-PT.

Fe<sub>3</sub>O<sub>4</sub>/PZN-PT heterostructures were also made in order to improve the microwave tunable range and reduce the FMR linewidth. A record high electric-field-induced FMR field shift up to 860 Oe was observed, corresponding to a ME coefficient of 108 Oe cm kV<sup>-1</sup> in the Fe<sub>3</sub>O<sub>4</sub>/PZN-PT heterostructures. In addition the FMR linewidth was reduced from 480–620 Oe in Fe<sub>3</sub>O<sub>4</sub>/PMN-PT to 330–380 Oe in Fe<sub>3</sub>O<sub>4</sub>/PZN-PT, leading to a

ratio of tunable FMR field over FMR linewidth of 2.5. It is notable that for microwave magnetic devices which operate near the FMR or directly use the FMR effect, the ratio of FMR field shift range over FMR linewidth is of paramount importance. We would also like to add that for many other tunable microwave magnetic devices which operate far away from the FMR effect, such as phase shifters, etc., a large tunable magnetic field range is more important. The giant electrostatic tunable FMR field and low synthesis temperature make these multiferroic heterostructures great candidates for applications in electrostatically tunable microwave multiferroic devices.

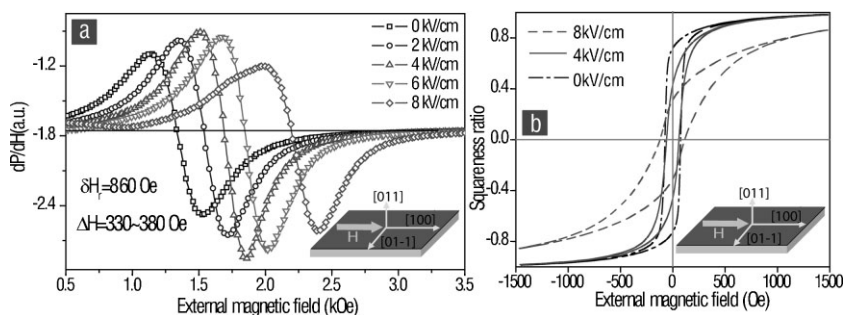


**Figure 7.** Ferromagnetic resonance absorption spectra of Fe<sub>3</sub>O<sub>4</sub>/PZN-PT (a) and magnetic hysteresis loops of Fe<sub>3</sub>O<sub>4</sub>/PZN-PT (b) while applying different electric fields.

## 4. Experimental

Multiferroic composite material  $\text{Fe}_3\text{O}_4/\text{PZT}$ ,  $\text{Fe}_3\text{O}_4/\text{PMN-PT}$ , and  $\text{Fe}_3\text{O}_4/\text{PZN-PT}$  were obtained by spin-spray deposition of  $\text{Fe}_3\text{O}_4$  ferrite on polycrystal PZT substrate with the dimension of  $15 \times 7 \times 0.5$  mm ( $L \times W \times H$ ), (011) cut single crystal PMN-PT substrate with dimensions of  $10 \times 5 \times 0.5$  mm ( $L \times W \times H$ ) and (011) cut single crystal PZN-PT substrate with dimensions of  $10 \times 5 \times 0.5$  mm ( $L \times W \times H$ ) at  $90^\circ\text{C}$ , respectively. The PZT, PMN-PT and PZN-PT slabs coated with electrodes on both sides were polarized under poling field of  $6 \text{ kV cm}^{-1}$  across the thickness direction before depositing the  $\text{Fe}_3\text{O}_4$  film. An  $\text{Fe}^{2+}$  aqueous solution (10 mmol) and a pH value of 4.0 was used as precursor solution for  $\text{Fe}_3\text{O}_4$  ferrite deposition. At the same time, an aqueous oxidation solution consisted of  $\text{NaNO}_2$  (2 mmol) and  $\text{CH}_3\text{COONa}$  (140 mmol) with a pH value of 8.5 was prepared. Through separate nozzles, these two reaction solutions were sprayed at a flow rate of  $40 \text{ mL min}^{-1}$  simultaneously onto a spinning hot PMN-PT and PZT substrates at  $90^\circ\text{C}$  with a rotation speed of 150 rpm.  $\text{N}_2$  gas was blown into the chamber to mitigate the  $\text{Fe}^{2+}$  oxidation effects from the oxygen in air. After thirty minutes plating, uniform  $\text{Fe}_3\text{O}_4$  films on PZT, PMN-PT and PZN-PT with strong adhesion and the were obtained with a growth rate of  $\sim 30 \text{ nm min}^{-1}$ .

The static ME coupling measurements were performed by vibrating sample magnetometry (VSM). The  $\text{Fe}_3\text{O}_4/\text{PZT}$ ,  $\text{Fe}_3\text{O}_4/\text{PMN-PT}$ , and  $\text{Fe}_3\text{O}_4/\text{PZN-PT}$  samples were mounted onto the VSM holder and the in-plane hysteresis loops were measured under various electric fields which were applied across the thickness of ferroelectric substrates coated with Cu as electrodes. Microwave ME interaction was investigated by an X-band ( $\sim 9.5 \text{ GHz}$ ) electron paramagnetic resonance (EPR) system with a TE<sub>102</sub> cavity. The static electric field was applied across the  $\text{Fe}_3\text{O}_4/\text{PZT}$ ,  $\text{Fe}_3\text{O}_4/\text{PMN-PT}$ , and  $\text{Fe}_3\text{O}_4/\text{PZN-PT}$  samples thickness direction. Both the external bias magnetic field and microwave magnetic field were applied orthogonal and in-plane of the  $\text{Fe}_3\text{O}_4$  film. The ferroelectric property of PMN-PT and PZT were measured by a Radiant RT-6000 ferroelectric testing station.

## Acknowledgements

This work is sponsored by NSF under awards ECCS-0746810, DMR-0603115, and ECCS-0824008, and the ONR Awards N000140710761 and N000140810526.

Received: October 13, 2008  
Revised: December 24, 2008  
Published online: April 8, 2009

[1] J. F. Scott, *Nat. Mater.* **2007**, *6*, 256.

- [2] M. Fiebig, *J. Phys. D* **2005**, *38*, R123.  
 [3] S. Shastry, G. Srinivasan, M. I. Bichurin, V. M. Petrov, A. S. Tatarenko, *Phys. Rev. B* **2004**, *70*, 064416.  
 [4] C. W. Nan, M. I. Bichurin, S. X. Dong, D. Viehland, *J. Appl. Phys.* **2008**, *103*, 031101.  
 [5] J. Zhai, Z. Xing, S. X. Dong, J. F. Li, D. Viehland, *Appl. Phys. Lett.* **2006**, *88*, 062510.  
 [6] W. Eerenstein, N. D. Mathur, J. F. Scott, *Nature* **2006**, *442*, 759.  
 [7] T. Lottermoser, T. Lonkai, U. Amann, D. Hohlwein, J. Ihringer, M. Fiebig, *Nature* **2004**, *430*, 541.  
 [8] S.-W. Cheong, M. Mostovoy, *Nat. Mater.* **2007**, *6*, 13.  
 [9] H. Zheng, J. Wang, S. E. Lofland, Z. Ma, L. Mohaddes-Ardabili, T. Zhao, L. Salamanca-Riba, S. R. Shinde, S. B. Ogale, F. Bai, D. Viehland, Y. Jia, D. G. Schlom, M. Wuttig, A. Roytburd, R. Ramesh, *Science* **2003**, *303*, 661.  
 [10] A. Brandlmaier, S. Geprägs, M. Weiler, A. Boger, M. Opel, *Phys. Rev. B* **2008**, *77*, 104445.  
 [11] M. Liu, X. Li, J. Lou, S. Zheng, K. Du, Nian, X. Sun, *J. Appl. Phys.* **2007**, *102*, 083911.  
 [12] J. Ma, Z. Shi, C. W. Nan, *Adv. Mater.* **2007**, *19*, 2571.  
 [13] C. Pettiford, S. Dasgupta, J. Lou, S. D. Yoon, N. X. Sun, *IEEE Trans. Magn.* **2007**, *43*, 3343.  
 [14] M. Liu, X. Li, H. Imrane, Y. Chen, T. Goodrich, K. S. Ziemer, J. Y. Huang, N. X. Sun, *Appl. Phys. Lett.* **2007**, *90*, 152501.  
 [15] A. S. Tatarenko, V. Gheevarghese, G. Srinivasan, *Electron. Lett.* **2006**, *42*, 540.  
 [16] Y. K. Fetisov, G. Srinivasana, *Appl. Phys. Lett.* **2006**, *88*, 143503.  
 [17] A. Ustinov, G. Srinivasan, B. A. Kalinikos, *Appl. Phys. Lett.* **2007**, *90*, 031913.  
 [18] J. Lou, R. E. Insignares, Z. Cai, K. S. Ziemer, M. Liu, N. X. Sun, *Appl. Phys. Lett.* **2007**, *91*, 18254.  
 [19] P. Han, W. Yan, J. Tian, X. Huang, H. Pan, *Appl. Phys. Lett.* **2005**, *86*, 052902.  
 [20] J. Lou, D. Reed, C. Pettiford, M. Liu, P. Han, S. X. Dong, N. X. Sun, *Appl. Phys. Lett.* **2008**, *92*, 262502.  
 [21] M. Abe, Y. Tamaura, *Jpn. J. Appl. Phys. Part 2* **1983**, *22*, L511.  
 [22] M. Abe, *Electrochim. Acta* **2000**, *45*, 3337.  
 [23] G. M. Yang, A. Daigle, M. Liu, O. Obi, S. Stoute, K. Naishadham, N. X. Sun, *Electron. Lett.* **2008**, *44*, 332.  
 [24] G. M. Yang, X. Xing, A. Daigle, M. Liu, O. Obi, J. W. Wang, K. Naishadham, N. X. Sun, *IEEE Trans. Magn.* **2008**, *44*, 3091.  
 [25] M. Liu, O. Obi, J. Lou, S. Stoute, J. Y. Huang, Z. Cai, K. S. Ziemer, N. X. Sun, *Appl. Phys. Lett.* **2008**, *92*, 152504.  
 [26] R. C. O'handley, in: *Modern Magnetic Materials: Principles and Applications*, Wiley, New York **2000**, Ch. 7.  
 [27] C. Thiele, K. Dörr, O. Bilani, J. Rödel, L. Schultz, *Phys. Rev. B* **2007**, *75*, 054408.